Geometrical characterization of hard-sphere systems

Patrick Richard,[1] Luc Oger,[1] Jean-Paul Troadec,[1] and Annie Gervois[2]
[1]*Groupe Matière Condensée et Matériaux, UMR CNRS 6626, Université de Rennes I, 35042 Rennes Cedex, France*
[2]*Service de Physique Théorique, Direction de Sciences de la Matière, CEA/Saclay, 91191 Gif-sur-Yvette Cedex, France*
(Received 19 February 1999)

By using molecular dynamics simulations on a large number of hard spheres and the Voronoï tessellation we characterize hard-sphere systems geometrically at any packing fraction η along the different branches of the phase diagram. Crystallization of disordered packings occurs only for a small range of packing fraction. For the other packing fractions the system behaves as either a fluid (stable or metastable) or a glass. We have studied the evolution of the statistics of the Voronoï tessellation during crystallization and characterized the apparition of order by an order parameter (Q_6) built from spherical harmonics. [S1063-651X(99)19510-2]

PACS number(s): 05.70.Fh, 05.20.−y, 61.20.−p

I. INTRODUCTION

Packings of hard spheres are convenient models to study many physical systems such as granular materials [1–4], simple liquids [5–8], colloidal suspensions [9,10], etc. The main advantage of this model is the simplicity of its interparticle potential Φ, which is defined by

$$\begin{aligned} \Phi &= \infty \quad \text{if} \quad r \leqslant 2R \\ \Phi &= 0 \quad \text{if} \quad r > 2R, \end{aligned} \tag{1}$$

where r is the distance between two centers of sphere and R the radius of the spheres. It is admitted that the packing fraction η of such packings (defined as the ratio of the volume occupied by the spheres to the total volume) cannot exceed $\pi/3\sqrt{2} \approx 0.74$, corresponding to compact ordered configurations [hexagonal close-packed (HCP) and face-centered cubic (FCC)]. One of the most striking properties of a hard-sphere system is the existence of a first order fluid-to-solid transition when the packing fraction increases [11–14]. It is possible to have disordered systems at packing fractions higher than the packing fraction of freezing, but they are metastable. The maximum packing fraction (the so-called random close packing, RCP) that such packings can reach is approximately $\eta_{RCP} \simeq 0.64$. This value is not an exact value as for compact ordered packings but an empirical one that varies slightly according to the authors [5,8,15].

In this paper, by using the Voronoï tessellation, we characterize geometrically hard-sphere systems obtained by numerical simulations along the different branches of the phase diagram and we study the crystallization of disordered packings. In Sec. II, we introduce the algorithms used to build the initial systems and our hard-sphere molecular dynamic algorithm. In Sec. III, we present the tools used to characterize the packing, i.e., the Voronoï tessellation and the bond order parameter. In Sec. IV, we report the phase diagram. The geometric properties of the packings along the different branches are described in Sec. V. In Sec. VI, we study the possible crystallization of disordered metastable packings, its effect on the geometric parameters during the crystallization and compare the informations given by the Voronoï tessellation and by the order parameter. Finally, in Sec. VII, we present our conclusions.

II. NUMERICAL PACKINGS

In this section, we first present the different methods used to build the initial packings of spheres, and then we describe the molecular dynamics algorithm used to equilibrate and eventually crystallize them. We start from nonequilibrated packings, ordered or disordered. To obtain an ordered packing, we simply decrease the radius of the spheres of a FCC packing to have the wanted packing fraction. A disordered packing is obtained using the Jodrey and Tory's algorithm [16]. It is based on an iterative sequential resorption of overlaps. The input parameters allow to control the final diameter of the sphere. As a consequence, we can build Jodrey-Tory's packing in a large range of packing fraction (from $\eta \approx 0.4$ to $\eta \approx 0.64$).

All the packings are made of approximately 15 000 spheres. Some larger packings with approximately 30 000 spheres were built to refine some peculiar data. Once the packing has been built, ordered or disordered, it is equilibrated and eventually crystallized using a molecular dynamics (event-driven) algorithm. We give a random initial velocity to each sphere, in such a way that the total momentum is equal to 0. The spheres move independently unless an event takes place. An event is an instantaneous elastic collision between two particles. It is characterized by a sudden change of particle momentum. Since the collisions are instantaneous, there are only binary collisions in the system. Our algorithm uses periodic boundary conditions. A general description of molecular dynamics of hard-sphere systems can be found in [17].

III. CHARACTERIZATION OF THE PACKINGS

A. Thermodynamical properties

The thermodynamical properties of elastic hard-sphere systems depend on the temperature in a trivial manner. Since the collisions are instantaneous, changing the temperature just rescales the time in the system.

Two methods can be used to calculate the pressure in the packing. The first one consists of calculating the collision rate Γ from which we can deduce the pressure by the formula

$$\frac{PV}{NkT}=1+\frac{\Gamma}{\Gamma_0}, \tag{2}$$

where P is the pressure, V the total volume, N the number of spheres, T the temperature, k the Boltzmann's constant, and $\Gamma_0=8\sqrt{\pi\langle v^2\rangle/3}R^2N(N-1)/V$ [18] is the low-density collision rate for large packings of hard spheres. In the expression of Γ_0, $\langle v^2\rangle$ is the mean square velocity. The second method is based on the fact that the equation of state of hard spheres is related to the radial distribution function $g(r)$ at contact $r=2R$, where R is the radius of the spheres,

$$\frac{PV}{NkT}=1+4\eta g(2R). \tag{3}$$

The two methods give close values, but the second one requires some care: $g(2R)$ is difficult to measure with precision since the radial distribution function can rise or fall rapidly close to $r=2R$. So we determine the pressure from the collision rate [Eq. (2)].

B. Geometric characterization of the packing

Our analysis of the geometry is based on a classic tool of the statistical geometry: the Voronoï tessellation of the packing [19]. This method is very powerful for studying correlations in packings of spheres [20,21], the structure of glasses [22,23], of Frank-Kasper phases [24], or of simple liquids and amorphous solids [25,26]. It can been generalized to polydisperse assemblies of spheres by using the Laguerre distance between spheres [27] or by using the Voronoï S-net [28]. One of its more recent and original uses is the study of the growth of cellular materials [29]. It has been already used by Tanemura *et al.* [30] in a geometrical analysis of crystallization. A Voronoï polyhedron of a sphere [31] contains all points in space that are closer to the sphere center than to all other particles. It is delimited by the smallest envelope of bisecting planes with the other spheres. The Voronoï tessellation is the whole collection of the Voronoï polyhedra. It creates a froth which may be considered without any reference to the underlying spheres [20]. It allows us to define the notion of ''neighbor'' without ambiguity for any packing fraction: two spheres are neighbor if their Voronoï polyhedra share one face.

The basic quantities we study in this paper are:

(i) the mean number $\langle f\rangle$ of faces of the Voronoï polyhedra,

(ii) the variance μ_2 of f: $\mu_2=\langle f^2\rangle-\langle f\rangle^2$,

(iii) the fraction p_i of faces that have i edges,

(iv) the slope of the Aboav-Weaire's law, which describes the topological correlation between neighbors. Let be $m(f)$, the average number of faces of the neighbors of a f-faceted cell. We have

$$m(f)=\langle f\rangle-a+\frac{\langle f\rangle a+\mu_2}{f}, \tag{4}$$

where a is a parameter (of order of 1), which depends on the nature of the foam.

C. The measure of the order

The classical way for determining order in an isotropic packing of spheres is by inspection of its radial distribution function. As the crystallization begins to occur, a very small peak appears for a value of r which corresponds to the second neighbors in a FCC or HCP arrangement, $r=2\sqrt{2}R$. As pointed out by Rintoul and Torquato [32], this method is unsatisfying for two reasons: on one hand the absence of the peak does not necessarily mean the absence of crystallization, and on the other hand it is very difficult to determine when the peak appears.

Steinhardt *et al.* [33] have proposed another way to determine more quantitatively order in a packing. The method consists of assigning the quantity

$$Q_{lm}=Y_{lm}(\theta(\vec{r}),\phi(\vec{r})) \tag{5}$$

to every ''bond'' joining a sphere to its neighbors, where $Y_{lm}(\theta(\vec{r}),\phi(\vec{r}))$ are spherical harmonics, each bond being identified by its midpoint $\vec{r}$ and its polar angles $\theta(\vec{r})$ and $\phi(\vec{r})$ measured in respect to some arbitrary reference coordinate system. The Q_{lm} depend on the reference coordinate system, so one must consider rotationally invariant combinations, such as

$$Q_l=\left(\frac{4\pi}{2l+1}\sum_{m=-l}^{l}|\langle Q_{lm}\rangle|^2\right)^{1/2}, \tag{6}$$

where $\langle Q_{lm}\rangle$ is the average of Q_{lm} over all bonds.

Since the lowest nonzero Q_l in common with the icosahedral symmetry and cubic symmetry corresponds to $l=6$ [33], Q_6 can be taken as an order parameter. Q_6 is very sensitive to any kind of crystallization and increases significantly when order appears. It is important to notice here that since Q_6 is calculated on the Voronoï neighbors, its value for a compact structure is lower than that calculated with only the nearest neighbors. For example, in the slightly disordered FCC case [34], there are 12 nearest neighbors placed at $2R$ and on average 14 Voronoï neighbors (the 12 nearest and, on average, 2 placed at $2\sqrt{2}R$). The value of Q_6 calculated on the nearest neighbors is 0.5745, whereas it is on average 0.454 on the Voronoï neighbors.

Another way to measure the local order of a packing of spheres is by way of the fractions p_i of i-edged faces of the tessellation [30,21,20]. Crystallized structures with a high degree of icosahedral order, such as the A15 structure (β-tungsten), have a high value of p_5 which decreases sharply when the melting occurs [24], while in structure where cubic symmetry dominates, p_6 and p_4 are high and abruptly decrease at melting. Then the study of the p_i's allows us to get an idea of the symmetry of a packing and to localize the structural phase transition.

IV. PHASE DIAGRAM

We have reported in Fig. 1 the phase diagram in the pressure-packing fraction plane. It is made of four branches: the fluid branch, the coexistence branch, the stable solid branch, and the metastable branch. The fluid branch starts at $\eta=0$ with the value $PV/NkT=1$ which corresponds to an ideal monoatomic gas. We obtain it by performing molecular

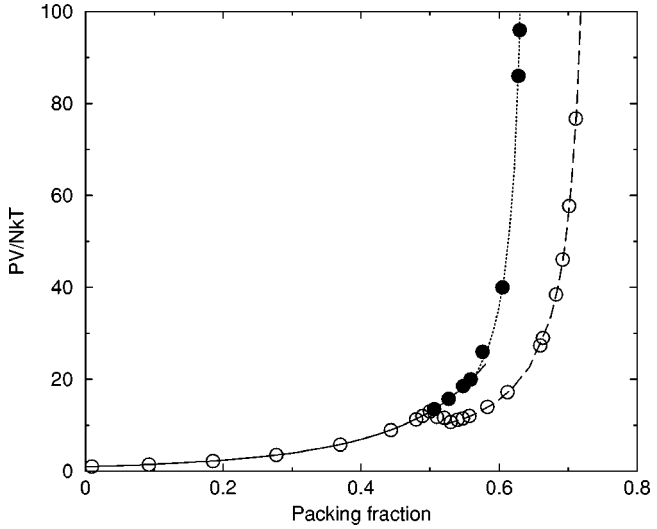

FIG. 1. Evolution of PV/NkT for thermodynamically stable (○) and metastable (●) packings. Solid line, Carnahan and Starling [35]; dotted line; Speedy [38]; dashed line; Hall [37].

simulations on FCC and Jodrey-Tory's packings of low packing fraction until the pressure reaches a constant value. As the packing fraction increases, the number of collisions per unit of time becomes more and more important and the pressure increases until the freezing point, which corresponds to a packing fraction $\eta_f \approx 0.495$. At this point the first order transition can occur and the branch splits into two parts: the coexistence branch and the metastable branch. A very good approximate expression for the fluid branch has been given by Carnahan and Starling [35]. The difference between this expression and our numerical data is less than 1%.

In the coexistence branch the fluid and the solid coexist in equilibrium at a given pressure until the melting point at the packing fraction $\eta_m \approx 0.545$. We do not observe a constant pressure but a ''Van der Waals loop'' consequence of the finite size of the system. This branch is obtained by performing molecular dynamics on FCC initial packings until the pressure reaches a constant value. The solid branch, obtained with FCC initial packings, is the stable branch of the system for packing fractions higher than the packing fraction of melting. The pressure goes to infinity when the packing fraction reaches the FCC value 0.7405. Our results are very close to those of Alder *et al.* [36]. A very good theoretical expression for this branch is given by Hall [37]. A small part of this branch can also be obtained by crystallization of a Jodrey-Tory's packing (see Sec. VI).

The last branch corresponds to the metastable state of the system for packing fraction higher than the packing fraction of freezing. The corresponding packings, obtained by equilibration of Jodrey-Tory's packings, are disordered and the pressure diverges when the packing fraction reaches the RCP value (≈ 0.64). The main difficulty in determining the pressure in this branch is to run the simulation long enough to equilibrate the packing without crystallizing it. For packing fractions between about 0.54 and 0.59, equilibration and crystallization are not well separated [38,32]: as seen in Fig. 2(a) we observe a short, slightly decreasing, plateau and then a faster decrease of the pressure, consequence of the crystallization; we take for the pressure the value of the small plateau. At higher packing fractions [Fig. 2(b)], the crystallization becomes more difficult; the pressure decreases first quickly because the initial packing is far from equilibrium; then it reaches a plateau value which we take as the pressure at the corresponding packing fraction for the metastable branch because there is no evident sign of crystallization (this will be confirmed by the measurement of Q_6; see the next section).

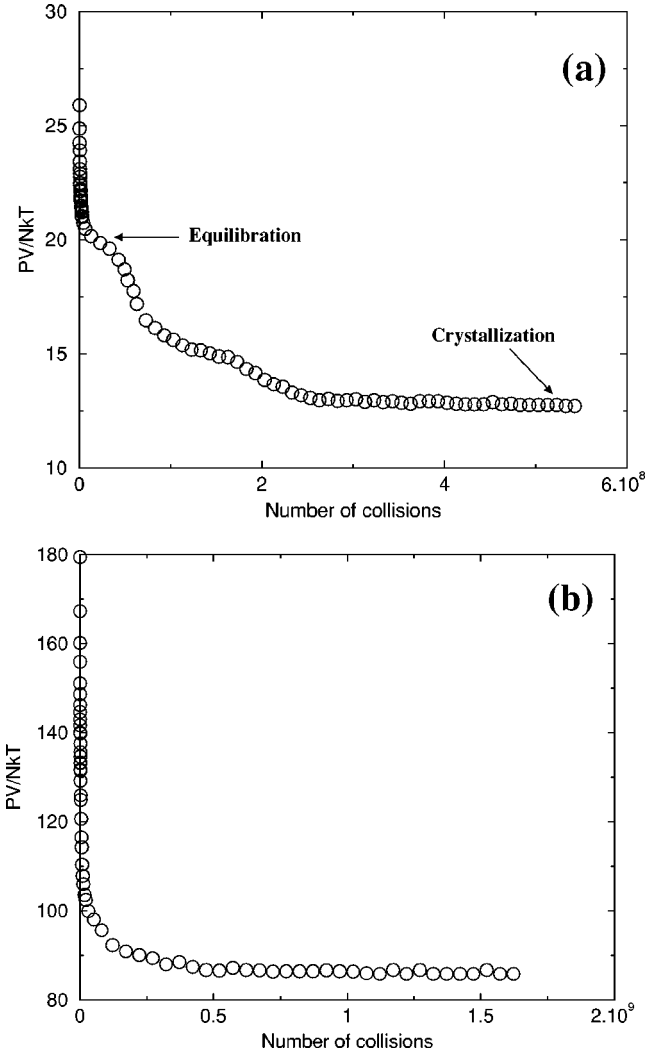

FIG. 2. PV/NkT as a function of the number of collisions for an initial Jodrey-Tory's packing of packing fraction $\eta = 0.558$ (a) and of packing fraction $\eta = 0.628$ (b).

Speedy [38] proposed an empirical equation of state for the metastable branch above $\eta = 0.56$ that fits very well our data. Another fit equation was given by Torquato [39].

V. GEOMETRICAL CHARACTERIZATION

In this section, we study the order parameter Q_6 and the topological parameters $\langle f \rangle$, μ_2, and p_i along the different branches of the phase diagram [Figs. 3, 4(a), 4(b), and 5]. For the p_i, we limit ourselves to the values obtained for $i = 4$, 5, and 6.

First, we note some common points in the evolution of all those quantities with the packing fraction. On the disordered

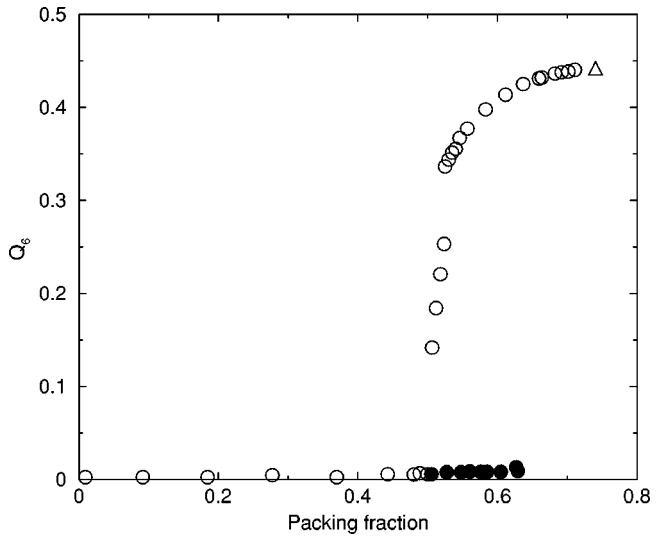

FIG. 3. The ''Q_6-phase diagram.'' (○), stable packings; (●), metastable packings; (△), theoretical value for the slightly disordered FCC.

branches, the variations are regular and we do not observe a notable modification of behavior when passing from the liquid branch to the metastable one. On the contrary, all the quantities show a sharp variation between the freezing point and the melting point (in fact this variation begins after the freezing point and stops before the melting point; this is due to the finite size of our system). Above the melting point, the variation is much slower.

We also note some significant features:

1. Q_6 gives really a measure of order in the packing. In the disordered branches, it is a very low sign of an absence of crystallization. It increases sharply in the coexistence branch, and continues to increase more slowly above melting, sign of a progressive structuration of the packing.

2. The average number of faces $\langle f \rangle$ decreases with the packing fraction starting from the exact value $\langle f \rangle = 48\pi^2/35+2 \simeq 15.535$ for $\eta=0$, obtained by Meijering [40]. For the crystallized packings, it is close to 14, the theoretical value for slightly disordered HCP or FCC packings [34]. For the random close packing, $\langle f \rangle$ is close to 14.2. The evolution of μ_2 is similar to that of $\langle f \rangle$; for the crystalline packings, μ_2 is almost constant ($\simeq 0.9$).

3. In the liquid and metastable branches, p_5 is continuously increasing with η; it is always larger than p_4 and p_6, sign of an important disorder in the packing. On the contrary, in the crystalline branch, p_6 is larger than p_5.

4. According to the Aboav-Weaire's law, the variations of the quantity $fm(f)$ with f can be fitted, with a good approximation, by a straight line for each packing fraction η. However, the slope $\kappa = \langle f \rangle - a$ of those lines depends on η, as already noted by Oger *et al.* [20]. From the variations of the topological quantities, we expect the Aboav-Weaire's law to be affected also by the degree of order in the packing. This is indeed the case as shown in Fig. 6. The variations of the slope κ are similar to those of the other quantities we have studied.

From above, it can be deduced that all the quantities we have considered can be used to characterize order in a packing of spheres. However, as can be seen in Figs. 3 to 6, the order parameter Q_6, which has very weak values in the disordered phases and much larger values in the crystalline phase, seems to be particularly suitable. This will be confirmed in the next section, where we consider the transition from the metastable branch to the crystalline branch.

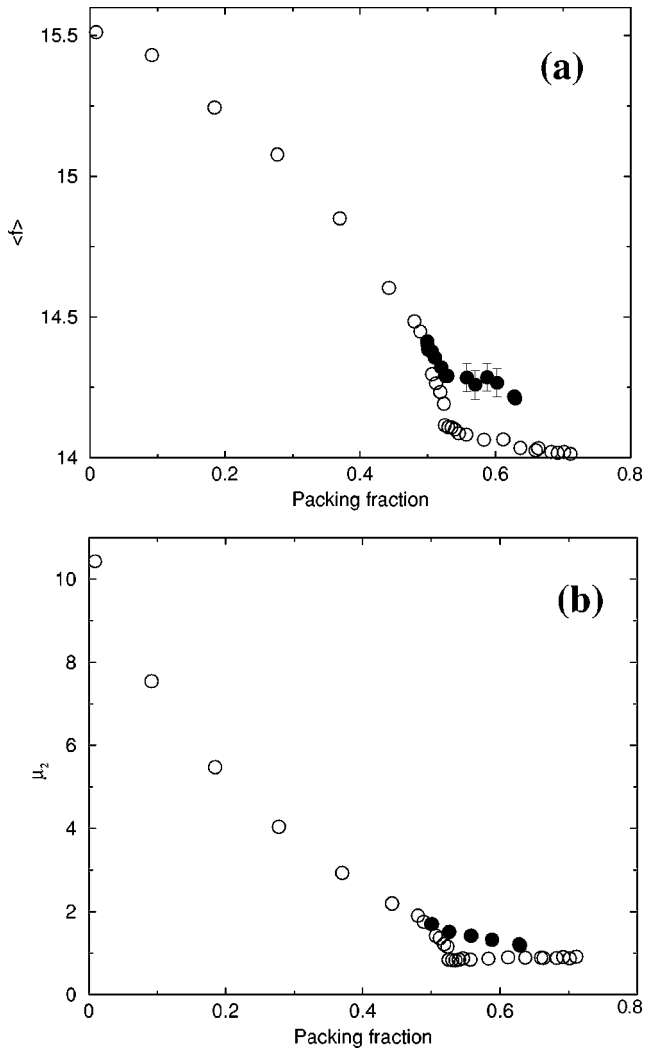

FIG. 4. $\langle f \rangle$ (a) and μ_2 (b) vs the packing fraction for the stable branches (○) and for the metastable branch (●). In (a) the error bars are given for the points corresponding to packing for which it is difficult to distinguish between equilibration and crystallization. For the other points, the errors are of the order of magnitude of the symbols. For (b) all the errors are smaller than the magnitude of the symbols.

VI. TRANSITION FROM THE METASTABLE BRANCH TO THE STABLE BRANCH

In this section we study the evolution of the geometrical quantities when a Jodrey-Tory packing with packing fraction between $\eta \simeq 0.545$ and $\eta \simeq 0.6$ [Fig. 7(a)] crystallizes [Fig. 7(b)].

A. Crystallization of the Jodrey-Tory's packings

The effects of the molecular dynamics algorithm on the Jodrey-Tory's packings depend strongly on the packing frac-

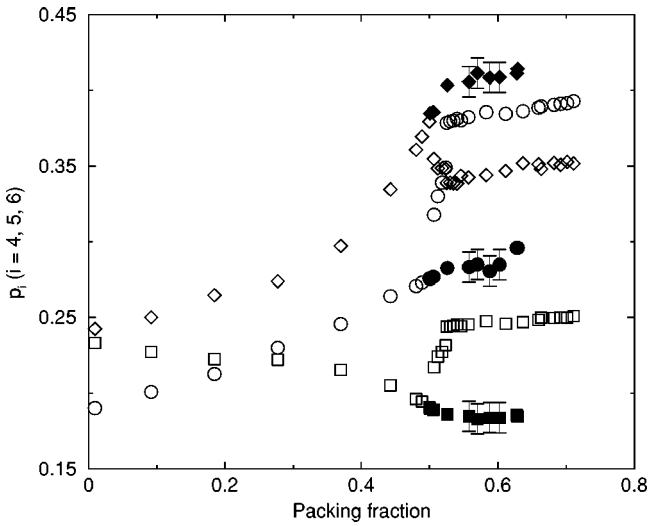

FIG. 5. Fraction p_i of faces having i edges vs the packing fraction p_4 (□), p5 (◇), p_6 (○). Open symbols: stable branches; closed symbols: metastable branch.

tion η. If one starts with a packing with η between $\eta_f = 0.495$ and $\eta_m = 0.545$ we do not observe crystallization, even after an important number of collisions (10^9 collisions); the system is a metastable fluid (the same behavior has been observed by Speedy [41]). Between η_m and η_{RCP}, an increase of packing fraction is synonymous of an increase of the difference of entropy between the ordered and the disordered state. So, one may think that the higher the packing fraction, the higher the propensity to crystallize. But, this propensity depends also on the free volume of the spheres. Indeed, if the spheres are very close to each other (i.e., at high packing fraction) their moves are very small and the structural reorganization very slow. The system is in a ''quenched'' state. This means that the competition between entropy and free volume governs the crystallization.

We have reported in Fig. 8 the evolution of Q_6 versus the packing fraction for initial Jodrey-Tory's packings after a given number of collisions (10^9) and in Fig. 9 the corresponding values of p_i. For comparison we have also reported the values of Q_6 for the stable branch and the values of p_i for the disordered packings. These figures clearly show that crystallization occurs only in a limited range of packing fractions. Moreover, in that range, the Q_6 values show that crystallization is not fully achieved after 10^9 collisions, although the pressure values (not shown) and the p_i values (compare Figs. 5 and 9) are close to their values in the crystalline branch. Here still, parameter Q_6 is a better measure of order than the other quantities. The propensity to crystallize is maximum for a packing fraction close to $\eta \simeq 0.58$. It is interesting to notice that it is very close to the value of the liquid-glass transition packing fraction determined numerically [42–44]. Furthermore, Fig. 8 shows that the structure of a crystallized hard sphere system is FCC.

As said above, at high packing fraction, the spheres cannot move easily and the crystallization cannot occur in rea-

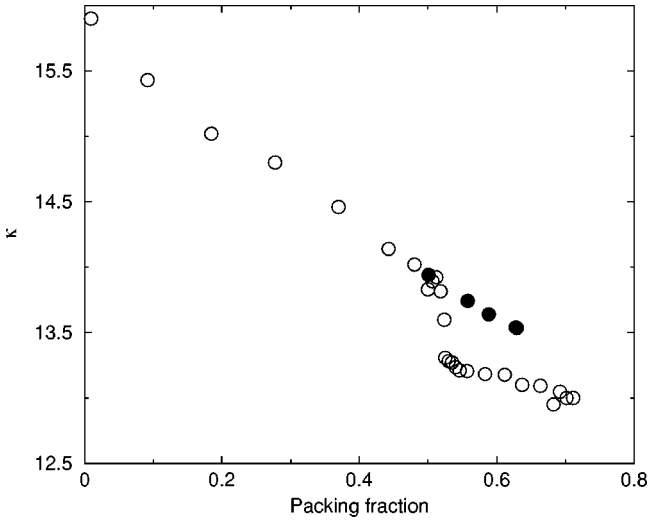

FIG. 6. Slope of $fm(f)$ vs the packing fraction for the stable branches (○) and for the metastable branch (●).

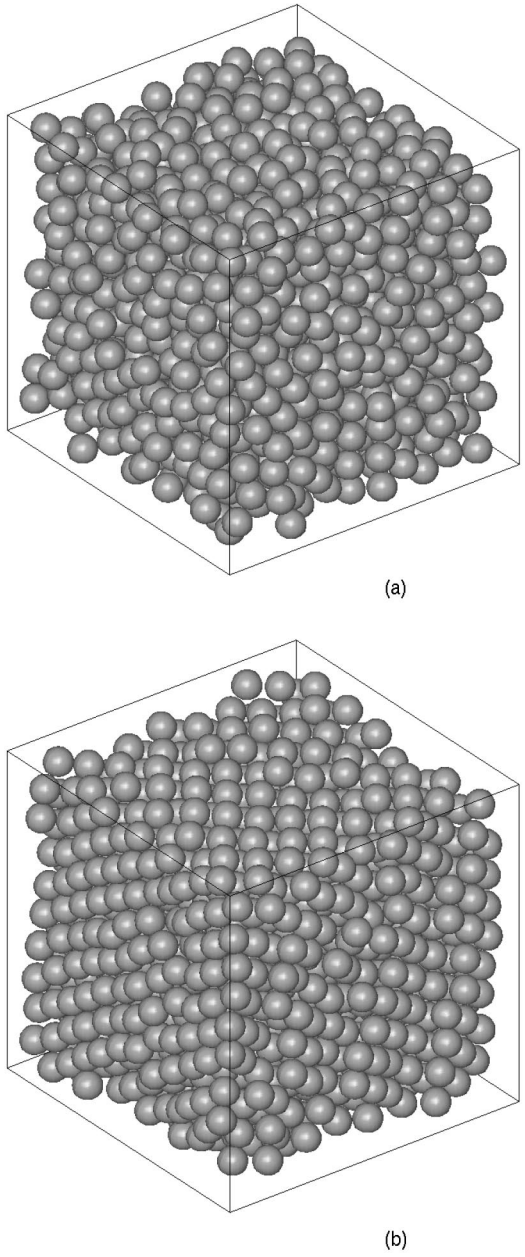

FIG. 7. Crystallization of an initially disordered packing of spheres with a packing fraction $\eta \simeq 0.558$. (a) part of the initial packing, (b) part of the packing after 10^9 collisions.

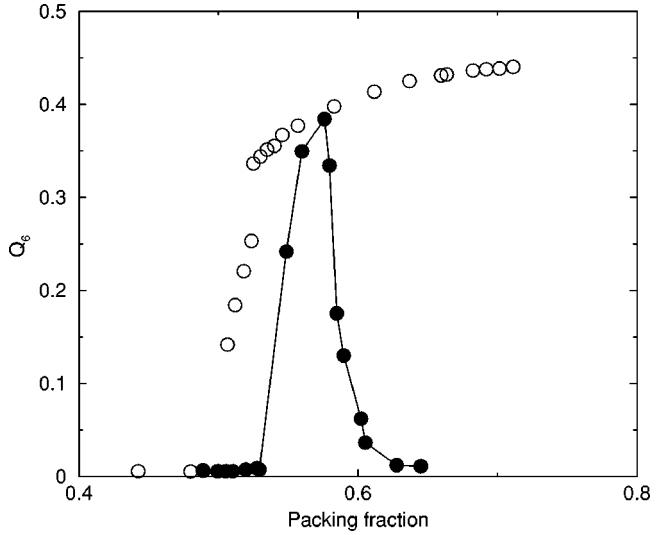

FIG. 8. Values of Q_6 for stable packings (○) and for initially metastable packings (●) after 10^9 collisions.

sonable times. Figure 2(b) illustrates our purpose for $\eta = 0.628$: the pressure reaches rapidly a plateau then decreases very slowly with time. After a very long time it could reach the value for the stable packing at the same packing fraction. The question of the existence of a glassy state for a packing of hard spheres is controversial [38,32,45,43]. Using the parameter Q_6, Rintoul and Torquato [32] found that, even at packing fraction as high as that of the RCP, small amounts of crystallization occur and the corresponding system is not in a glassy state.

We do not find clear sign of crystallization on packings corresponding to our ''glassy'' systems. We are then in agreement with a lot of previous authors [42,38,41,43]. Indeed, the values of Q_6 for these packings during all the dynamics do not vary significantly. Furthermore the examination of Figs. 8, 9, and 2(a) shows clearly the existence of a system which has the local structure of a liquid and which reorganizes itself very slowly with time. So our numerical

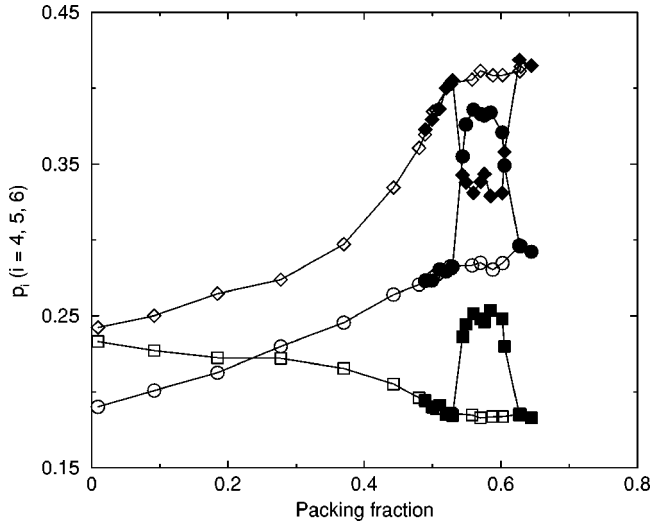

FIG. 9. Values of p_4 (□), p_5 (◇), and p_6 (○) for disordered packings (open symbols) and for initially metastable packings after 10^9 collisions (closed symbol).

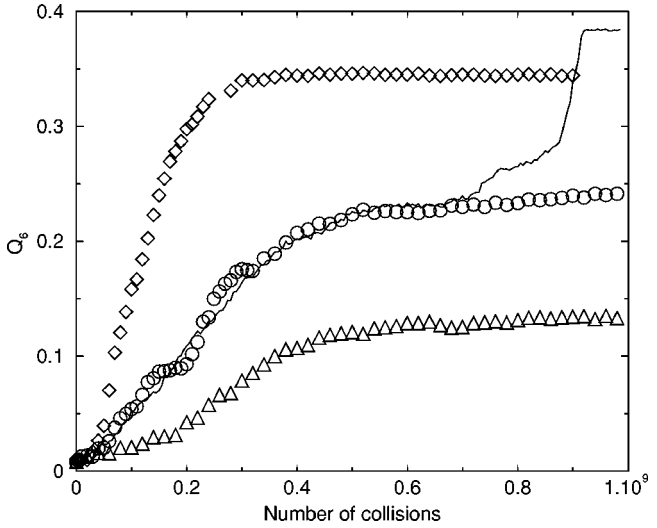

FIG. 10. Evolution of Q_6 with the number of collisions for initial Jodrey-Tory's packings. $\eta = 0.548$ (○), $\eta = 0.558$ (◇), $\eta = 0.576$ (−), and $\eta = 0.585$ (△).

simulations seem to show the existence at high packing fractions of a metastable glassy state.

B. Evolution of the geometry of the packing with packings belonging initially to the metastable branch

We have studied the evolution of all the geometrical quantities defined previously, with the number of collisions for Jodrey-Tory's packings with packing fraction allowing partial crystallization. We have reported in Fig. 10 the evolution of Q_6 with the number of collisions for 4 values of the packing fraction. We observe that Q_6 increases with the number of collisions, sign of a crystallization. At some times, the evolution of Q_6 can be very sharp corresponding to strong and global reorganizations.

We have reported in Fig. 11 the evolution of $\langle f \rangle$ with the number of collisions for a packing with $\eta = 0.558$. After a sharp initial variation, $\langle f \rangle$ decreases slowly with the number of collisions from 14.38 to 14.08, which is

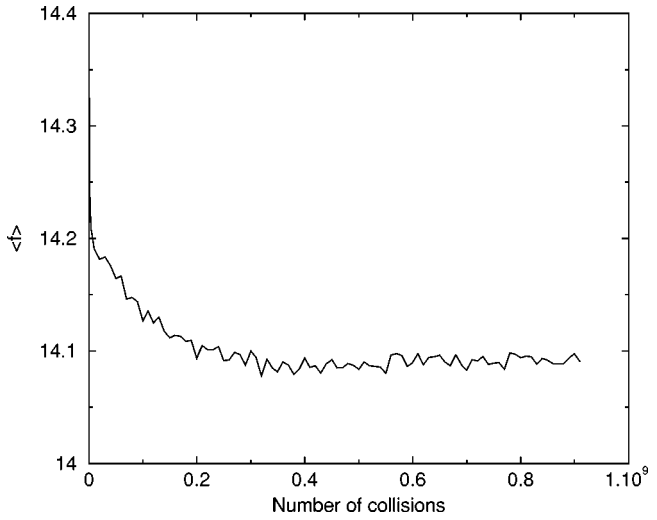

FIG. 11. $\langle f \rangle$ vs the number of collisions for the crystallization of a Jodrey-Tory's packing with a packing fraction of 0.558.

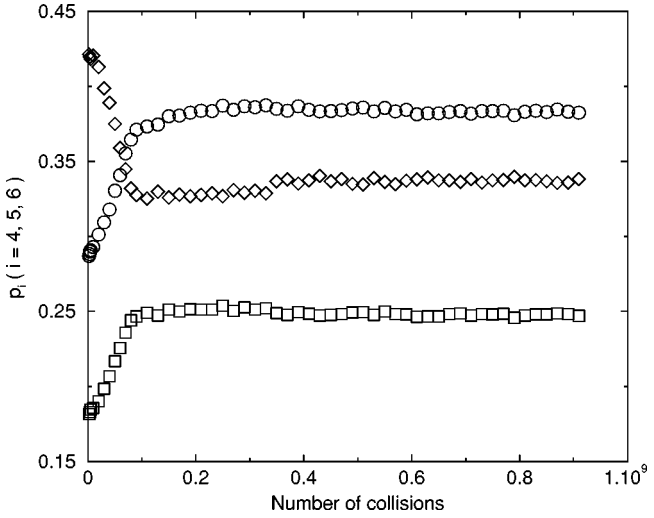

FIG. 12. Fraction of faces haven i edges versus the number of collisions for a packing fraction of 0.558 p_4 (□), p_5 (◇), and p_6 (○).

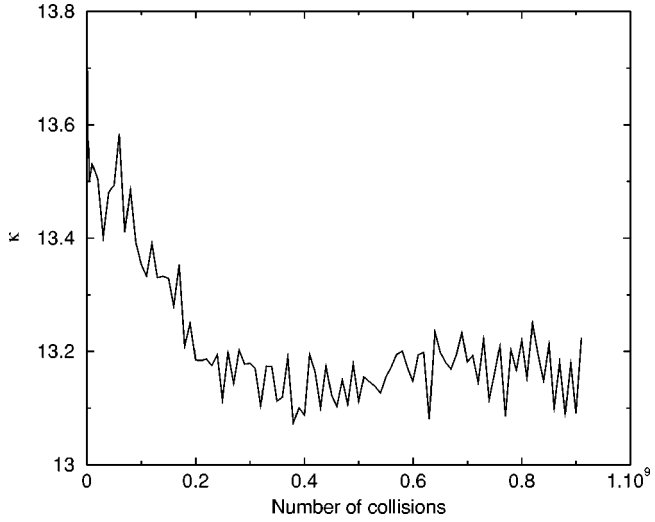

FIG. 14. Slope κ of $fm(f)$ vs the number of collisions for an initial Jodrey-Tory's packing with a packing fraction of 0.558.

very close to the corresponding value of the crystalline branch. The evolution of μ_2 is very similar: it decreases from 1.27 to 0.93.

The evolution of p_4, p_5, and p_6 with the number of collisions is represented in Fig. 12 for $\eta=0.558$. We observe a short variation and then a steady state. A $t=0$ we have a large number of five-edged faces ($\approx 43\%$), whereas the number of four and six-edged faces are lower (respectively $\approx 18\%$ and 28%). When crystallization occurs the number of disclinations increases, and the number of pentagonal faces decreases.

The topological parameters (and also the pressure, which is not shown) reach rapidly steady values, close to their values in the crystalline branch. In the same time, Q_6 continues to increase (Fig. 10). One more time, we are led to the conclusion that Q_6 is a more precise measure of the configuration of the spheres. To illustrate this purpose, we have reported in Fig. 13 the evolution of Q_6 with p_6 during the relaxation of Jodrey-Tory packings at different packing fractions. We see that p_6 is rapidly close to its final value, whereas at this moment the value of Q_6 is almost four times lower than its final value.

As is shown in Fig. 14, the slope of the Aboav-Weaire's law, κ, decreases slightly with the number of collisions. In fact the difference between the values of κ for disordered and for ordered packings is weak (Fig. 15). So, the modification of the Aboav-Weaire's law during crystallization is very weak.

VII. CONCLUSION

We have studied the phase diagram of hard-sphere systems not only from a thermodynamical point of view, but also from a geometrical point of view. This was done by combining the Voronoï tessellation and classical hard-sphere molecular simulations. The different topological properties for the four branches of the hard-sphere phase diagram are presented in detail. We have shown that many of these properties are characteristic of the ''state'' of the packing. In

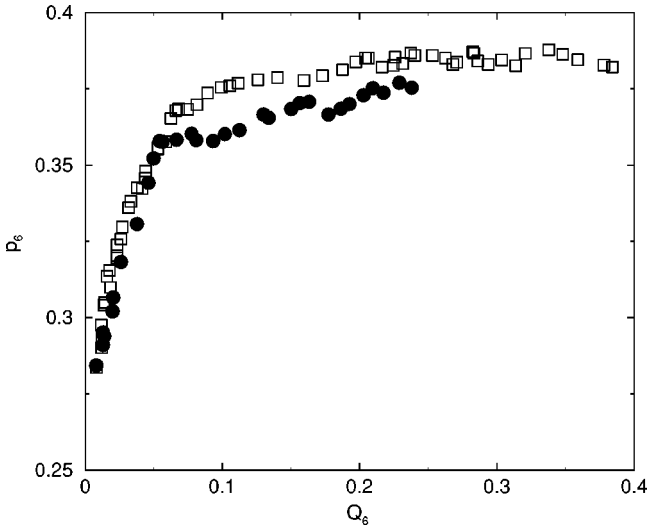

FIG. 13. p_6 vs Q_6 at different times during the Event-Driven simulation. $\eta=0.576$ (□), $\eta=0.548$ (●).

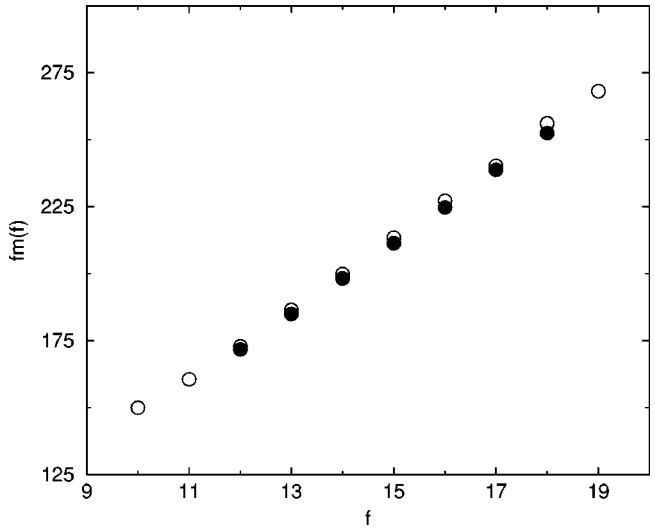

FIG. 15. $fm(f)$ for a packing of 16384 spheres of packing fraction $\eta\approx 0.558$. (●) after 10^9 collisions, (○) after 10^7 collisions.

particular, the average coordination number is lower for the crystallized branch than for metastable disordered branch and the fraction of five-edged faces is higher for the metastable branch than for the crystallized branch. We have also considered the evolution of the Voronoï parameters during the crystallization. They are good tools to investigate the order to disorder phase transition. But a more precise measure of order is given by the order parameter Q_6. The study of the evolution of the Q_6 with time shows that crystallization is only possible for a given range of packing fraction. Below this range we obtain a metastable fluid and above this range we obtain a glassy state.

ACKNOWLEDGMENTS

We would like to thank James T. Jenkins for stimulating discussions. We acknowledge the financial support from the CNRS and the NSF under Contract No. CNRS/NSF 409617.

[1] *Physics of Granular Media*, edited by D. Bideau and J. Dodds (Nova Science Publishers, New York, 1991).
[2] I. Goldhirsch and G. Zanetti, Phys. Rev. Lett. **70**, 1619 (1993).
[3] S. McNamara and W. Young, Phys. Rev. E **53**, 5089 (1996).
[4] S. Luding, E. Clément, J. Rajchenbach, and J. Duran, Europhys. Lett. **36**, 247 (1996).
[5] J.D. Bernal, Nature (London) **183**, 141 (1959).
[6] J.D. Bernal and J. Mason, Nature (London) **188**, 910 (1960).
[7] G.D. Scott, Nature (London) **188**, 908 (1960).
[8] J.L. Finney, Proc. R. Soc. London, Ser. A **419**, 479 (1970).
[9] P.N. Pusey, in *Liquids, Freezing and Glass Transition* edited by J.P. Hansen, D. Levesque, and J. Zinn-Justin (Elsevier, New York, 1993), pp. 763–931.
[10] M.A. Rutgers, J.H. Dunsmuir, J.Z. Xue, W.B. Russel, and P.M. Chaikin, Phys. Rev. B **53**, 5043 (1996).
[11] B.J. Alder and T.E. Wainwright, J. Chem. Phys. **27**, 1208 (1957).
[12] W.W. Wood and J.D. Jacobson, J. Chem. Phys. **27**, 1207 (1957).
[13] W.G. Hoover and F.H. Ree, J. Chem. Phys. **49**, 3609 (1968).
[14] H. Reiss and A.D. Hammmerich, J. Phys. Chem. **90**, 6252 (1986).
[15] J.G. Berryman, Phys. Rev. A **27**, 1053 (1983).
[16] W.S. Jodrey and E.M. Tory, Phys. Rev. A **32**, 2347 (1985).
[17] M.P. Allen and D.J. Tildesley, *Computer Simulation of Liquids* (Oxford University Press, New York, 1987).
[18] W.G. Hoover and B.J. Alder, J. Chem. Phys. **46**, 686 (1967).
[19] G.F. Voronoï, J. Reine Angew. Math. **134**, 198 (1908).
[20] L. Oger, A. Gervois, J.P. Troadec, and N. Rivier, Philos. Mag. B **74**, 177 (1996).
[21] R. Jullien, P. Jund, D. Caprion, and D. Quitman, Phys. Rev. E **54**, 6035 (1996).
[22] P. Jund, D. Caprion, and R. Jullien, Europhys. Lett. **37**, 547 (1997).
[23] Y. Hiwatari, T. Saito, and A. Ueda, J. Chem. Phys. **81**, 6044 (1984).
[24] P. Jund, D. Caprion, J.F. Sadoc, and R. Jullien, J. Phys.: Condens. Matter **9**, 4051 (1997).
[25] V.P. Voloshin, N.N. Medvedev, and Y.I. Naberukin, J. Struct. Chem. **28**, 216 (1987).
[26] V.A. Luchnikov, N.N. Medvedev, A. Appelhagen, and A. Geiger, Mol. Phys. **88**, 1337 (1996).
[27] P. Richard, L. Oger, J.P. Troadec, and A. Gervois, Physica A **259**, 205 (1998).
[28] N.N. Medvedev, Dokl. Phys. Chem. **337**, 767 (1994).
[29] N. Pittet, J. Phys. A **32**, 4611 (1999).
[30] M. Tanemura, Y. Hiwatari, H. Matsuda, T. Ogawa, N. Ogita, and A. Ueda, Prog. Theor. Phys. **58**, 1079 (1977)
[31] C.A. Rogers, *Packing and Covering* (Cambridge University Press, Cambridge, England, 1964).
[32] M. D. Rintoul and S. Torquato, J. Chem. Phys. **105**, 9258 (1996).
[33] P.J. Steinhardt, D.R. Nelson, and M. Ronchetti, Phys. Rev. B **28**, 784 (1983).
[34] J.P. Troadec, A. Gervois, and L. Oger, Europhys. Lett. **42**, 167 (1998).
[35] N.F. Carnahan and K.E. Starling, J. Chem. Phys. **51**, 635 (1969).
[36] B.J. Alder, W.G. Hoover, and D.A. Young, J. Chem. Phys. **49**, 3688 (1968).
[37] K.R. Hall, J. Chem. Phys. **57**, 2252 (1972).
[38] R.J. Speedy, J. Chem. Phys. **100**, 6684 (1994).
[39] S. Torquato, Phys. Rev. E **51**, 3170 (1995).
[40] J.L. Meijering, Philips Res. Rep. **8**, 270 (1953).
[41] R.J. Speedy, J. Phys.: Condens. Matter **9**, 8591 (1997).
[42] L.V. Woodcock, Ann. (N.Y.) Acad. Sci. **37**, 275 (1981).
[43] R.J. Speedy, Mol. Phys. **95**, 169 (1998).
[44] J.M. Gordon, J.H. Gibbs, and P.D. Fleming, J. Chem. Phys. **65**, 2771 (1976).
[45] M. Robles, M. Lopez de Haro, A. Santos, and S. Bravo Yuste, J. Chem. Phys. **108**, 1290 (1998).